Beyond Points: Evaluating Recent 3D Scan-Matching Algorithms

Martin Magnusson,[1] Narunas Vaskevicius,[2] Todor Stoyanov,[1] Kaustubh Pathak,[2] and Andreas Birk[2]

***Abstract*— Given that 3D scan matching is such a central part of the perception pipeline for robots, thorough and large-scale investigations of scan matching performance are still surprisingly few. A crucial part of the scientific method is to perform experiments that can be replicated by other researchers in order to compare different results. In light of this fact, this paper presents a thorough comparison of 3D scan registration algorithms using a recently published benchmark protocol which makes use of a publicly available challenging data set that covers a wide range of environments. In particular, we evaluate two types of recent 3D registration algorithms – one local and one global. Both approaches take local surface structure into account, rather than matching individual points. After well over 100 000 individual tests, we conclude that algorithms using the normal distributions transform (NDT) provides accurate results compared to a modern implementation of the iterative closest point (ICP) method, when faced with scan data that has little overlap and weak geometric structure. We also demonstrate that the minimally uncertain maximum consensus (MUMC) algorithm provides accurate results in structured environments without needing an initial guess, and that it provides useful measures to detect whether it has succeeded or not. We also propose two amendments to the experimental protocol, in order to provide more valuable results in future implementations.**

I. Introduction

Three-dimensional registration, or scan matching, is a crucial component of several robotics applications, such as mapping, object detection, manipulation, etc. Scan registration can be formulated as the problem of finding the relative transformation betwen two 3D point clouds that best aligns them.

A common problem with research papers presenting novel scan matching algorithms is that results are computed over a small number of scans from an application-specific environment. The need for standardised datasets for benchmarking registration algorithms has been recognised by the community and several recent works have been proposed [14, 10, 13]. However, in order to obtain the full benefits of such benchmarking efforts, it is critical that a sufficient number of registration algorithms are evaluated in a systematic manner, which is often not the case.

In this work we evaluate several recent registration algorithms on the challenging benchmarking dataset proposed by Pomerleau et al. [20]. We use this benchmark on two types of scan matching algorithms: local registration using NDT [11, 24] as well as the MUMC [15] algorithm for global matching. The purpose of this evaluation is two-fold: first, it aids the establishment of a scientific approach to comparing registration algorithms; and second, by applying a benchmark dataset and protocol designed originally for ICP-based algorithms to NDT and MUMC, we can identify the general validity of the proposed benchmark.

The two types of methods evaluated in this paper have different characteristics: MUMC decouples rotation and translation determination and does a global exhaustive search for the best alignment, while NDT registration uses local hill-climbing from an initial pose estimate. What is common for our algorithms is that they all take into account local surface structure around each point, and do not match individual points, in contrast to common ICP variants.

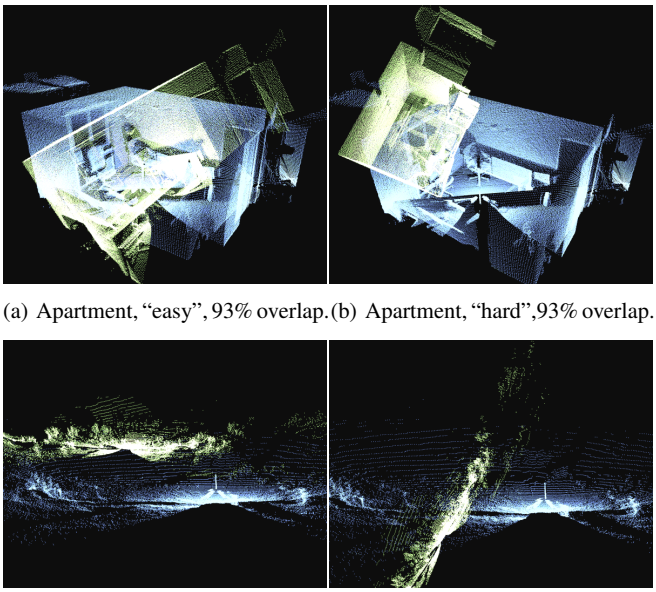

(a) Apartment, "easy", 93% overlap. (b) Apartment, "hard", 93% overlap.

(c) Plain, "easy", 37% overlap. (d) Plain, "hard", 37% overlap.

Fig. 1: Examples from the data sets.

The main contribution of the present paper is a thorough evaluation of these recent registration algorithms on a scale that has not previously been attempted, using 210 scan pairs from different types of environments, over 100 000 registrations in total. We show that both NDT and MUMC achieve more robust registration than ICP indoors, and that NDT performs well also outdoors. In addition, we show that the Distribution-to-Distribution variant of NDT (D2D-NDT [23]) is significantly faster than the others, though slightly less robust than Point-to-Distribution variant (P2D-NDT[11]). Furthermore, the present evaluation is the first one using the proposed protocol for non-ICP methods.

A second major finding of this paper is that the proposed benchmark [20] has significant shortcomings. First, the selection of unique scan pairs from the datasets is small, thus limiting the applicability for global scan matching approaches like MUMC. Second, the initial offsets provided are often unrealistic, while the amount of scan overlap is generally low. While this does indeed make the dataset more challenging, it limits its discriminative power in practically more interesting cases.

In addition to these main contributions, this article also presents several recent advances for NDT registration and makes available a new open-source implementation of the P2D-NDT algorithm.

II. Related work

Recently, much effort has been devoted to the benchmarking of 3D scan-registration and 3D SLAM algorithms. Different benchmarking approaches differ in the types of scenarios, the sensor

[1]Center of Applied Autonomous Sensor Systems (AASS), Örebro University, Sweden. firstname.lastname@oru.se

[2]Deptartment of EECS, Jacobs University, Bremen, Germany. f.lastname@jacobs-university.de

This work was funded in part by the EU FP7 projects SPENCER (ICT-2011-600877) and ROBLOG (ICT-270350), and the Swedish KK foundation under contract number 20110214 (ALLO).

used, and the kinds of ground-truth information available. In this discussion, we restrict ourselves to 3D mapping benchmarks – as opposed to the more common 2D benchmarks such as RADISH [7] and RAWSEEDS [4].

A good collection of 3D datasets is provided at [13]. The majority have been collected using a high-resolution, long-range, and large field-of-view Riegl VZ-400 scanner. In some cases, ground truth computed by manual registration using markers is provided. Some datasets have additional information like co-calibrated thermal and color data, and odometry. One of these datasets was used in Pathak et al. [14] to benchmark the performance of MUMC [15] and ICP. Most datasets in [13] are from outdoor urban scenarios. No protocol is defined to systematically evaluate new algorithms.

In Wulf et al. [26], a 1.2 km path in an outdoor urban (mostly flat) scene was captured in 924 scans of the RTS/ScanDriveDuo. A 2D ground-truth map was obtained from the land-registry office, and Monte Carlo localization (MCL) was used to compare the results of four 6D-SLAM strategies against this 2D reference, and some manual intervention was applied for quality control. The obvious limitation of this benchmark is the lack of full 3D ground-truth and providing only one type of environment.

Some authors have performed detailed studies of the "valleys of convergence" for registration algorithms [12, 10, 6], though typically only for a few scan pairs.

A tiltable SICK LMS 200 was employed in [10] to collect scans in an underground mining scenario. The two algorithms compared were ICP and NDT. No ground-truth was available, so the algorithms are compared with respect to accumulation of errors and the valley of convergence.

The common drawback of all the above mentioned benchmarks is the availability of only a single kind of environment and of typically only a few scan pairs. In contrast, the ETH benchmark used here [19, 20] has a range of environments, 6×35 scan pairs (chosen to have a uniform range of overlaps between 30% and 99%), with 3×64 pose offsets, sampled from a 6-DOF normal distribution. Hence, (for local registration methods at least) we have 40,320 tests in total for the benchmark, per algorithm.

III. Registration algorithms

Let $\mathcal{F}$ and $\mathcal{M}$ be two partially overlapping point clouds, taken from nearby poses. Additionally, we define $\mathcal{F}$ to be a *fixed* (or reference) scan, while $\mathcal{M}$ is a *moving* (or reading) point set. The registration task estimates the parameters Θ of a transformation function T, such that $T(\mathcal{M}, \Theta)$ is consistently aligned with $\mathcal{F}$.

A. P2D-NDT

The Normal Distributions Transform was originally developed in the context of 2D laser scan registration [2]. The central idea is to represent the observed range points as a set of Gaussian probability distributions. Assuming that a set of n point samples $\mathcal{P} = \{\boldsymbol{p}_i = (x_i, y_i, z_i)\}$ has been drawn from a Gaussian distribution $\mathcal{N}(\boldsymbol{\mu}, \Sigma)$, the maximum-likelihood estimates of the covariance and mean can be obtained from the observations:

$$\boldsymbol{\mu} = \frac{1}{n}\sum_{i=1}^{i=n} \boldsymbol{p}_i, \quad M = [\boldsymbol{p}_1 - \boldsymbol{\mu} \ldots \boldsymbol{p}_n - \boldsymbol{\mu}], \quad \Sigma = \frac{1}{n-1} M M^T$$

The probability density function estimated in this manner might or might not be a good representation of the sampled points, depending on the extent to which the Gaussian assumption on $\mathcal{P}$ holds. At a sufficiently small scale, a normal distribution can be considered a good estimate of local surface shape, in that it can represent planar and linear patches. Thus, the basic principle of the NDT is to represent space using a *set* of Gaussian probability distributions.

The point-to-distribution (P2D) variant of NDT for 3D registration [9] maximises the likelihood of points from one scan, given the NDT model created from the reference $M_{NDT}(\mathcal{F})$. The likelihood that a point $\boldsymbol{x}$ is generated from $M_{NDT}(\mathcal{F})$ is then:

$$p(\boldsymbol{x}|M_{NDT}(\mathcal{F})) = \sum_{i=1}^{n_{\mathcal{F}}} w_i \mathcal{N}(\boldsymbol{x}|\boldsymbol{\mu_i}, \Sigma_i), \tag{1}$$

where $n_{\mathcal{F}}$ is the number of Gaussian components of the 3D-NDT model of point cloud $\mathcal{F}$. The weight of each Gaussian component w_i determines the influence of that component in the model set on the likelihood of a single point from the moving scan. Magnusson et al. [11] propose to use trilinear interpolation in order to take into account neighbouring Gaussians. The implementation used in this work, however, only considers the closest Gaussian to each point, thus setting w_i to zero for all other Gaussians. P2D-NDT minimises an approximation of the negative log likelihood function of $p(T(\mathcal{M}, \Theta)|M_{NDT}(\mathcal{F}))$, over the space of transformation parameters Θ. After re-organisation of terms, the registration problem is posed as minimising the objective function

$$f_{p2d}(\Theta) = \sum_{j=1}^{|\mathcal{M}|} -d_1 \exp \frac{-d_2}{2} \hat{\boldsymbol{m}}_{\boldsymbol{j}}{}^T \Sigma_m^{-1} \hat{\boldsymbol{m}}_{\boldsymbol{j}}, \tag{2}$$

where d_1 and d_2 are positive regularizing factors (values are calculated based on the current NDT model resolution as described in [8, 3]), j iterates over all points $\boldsymbol{m}_j$ in the moving scan $\mathcal{M}$, $(\boldsymbol{\mu_m}, \Sigma_m)$ are the parameters of the corresponding closest normal distribution in $M_{NDT}(\mathcal{F})$, and $\hat{\boldsymbol{m}}_{\boldsymbol{j}} = T(\boldsymbol{m_j}, \Theta) - \boldsymbol{\mu_m}$. The objective f_{p2d} is doubly differentiable with analytic expressions for the gradient and Hessian. Once $\mathcal{M}_{NDT}$ has been constructed, 3D registration can be performed by minimizing the objective function (2) using a numerical optimization technique, such as Newton's method.

The P2D-NDT implementation used here also employs a regularization step to avoid near singular Hessian matrices in the optimisation step. The procedure is the same as for the D2D-NDT algorithm, and is further described in Section III-B.

Important Parameters: In this work, the P2D-NDT implementation is a recent re-implementation as part of the `perception_oru` suite[1]. Several parameters govern the performance of the algorithm:

- **Discretization levels:** the algorithm performs registration on models reconstructed at different spatial resolutions. Typically, it is desirable to first register at a coarse resolution (e.g. 2 m cells), followed by finer registration steps (e.g., 1 m and 0.5 m). Note that the solver may go from finer to coarser grids, and back again, in a similar fashion as is common in multigrid methods for solving linear systems.
- **Maximum number of iterations:** controls the number of optimization iterations allowed at each resolution.
- **Subsampling grid size:** in order to avoid bias from uneven point distribution and to speed up computations, the moving scan $\mathcal{M}$ is subsampled using a regular grid of a given resolution. This resolution is another important parameter which affects overall performance.

The parameter selection is summarized in Table I.

[1] http://wiki.ros.org/perception_oru

B. D2D-NDT

The Distribution-to-Distribution (D2D) variant of the NDT registration algorithm, proposed by Stoyanov et al. [23], is an extension of P2D-NDT which operates solely on NDT models. The algorithm minimizes the sum of L_2 distances between pairs of Gaussian distributions in two NDT models. Formally, the transformation between two point sets $\mathcal{M}$ and $\mathcal{F}$ is found by minimizing:

$$f(\Theta) = \sum_{i=1,j=i}^{n_{\mathcal{M}},n_{\mathcal{F}}} -d_1 \exp\left(-\frac{d_2}{2}\boldsymbol{\mu_{ij}}^T (R^T C_i R + C_j)^{-1} \boldsymbol{\mu_{ij}}\right) \tag{3}$$

over the transformation parameters Θ, where: $n_{\mathcal{M}}$ and $n_{\mathcal{F}}$ are the number of Gaussian components in the NDT models of $\mathcal{M}$ and $\mathcal{F}$; R and $\boldsymbol{t}$ are the rotation and translation components of Θ; $\boldsymbol{\mu}_i, C_i$ are the mean and covariance of each Gaussian component; $\boldsymbol{\mu_{ij}} = R\boldsymbol{\mu_i} + \boldsymbol{t} - \boldsymbol{\mu_j}$ is the transformed mean vector distance; and d_1, d_2 are regularization factors (fixed values of $d_1 = 1$ and $d_2 = 0.05$ were used). The optimization over Θ can be done efficiently using Newton optimization with analytically computed derivatives.

Two modifications of the D2D-NDT algorithm, compared to the previously published version [23], have been included in this work. The prior version only considered the sum of pairwise closest Gaussian components when forming the objective function in Eq. (3), while the version tested here can be configured to use a neighbourhood of close components. The second modification is the addition of a regularization step to the computation of the Hessian matrix, prior to the computation of a Newton step. We perform an eigen-decomposition of $H = Q\Lambda Q^{-1}$ and check if the smallest eigenvalue λ_{min} is close to 0. If that is the case, we compute a regularized Hessian matrix $H_r = Q(\Lambda + diag(\lambda_r))Q^{-1}$, where $\lambda_r = 10^{-3}\lambda_{max} - \lambda_{min}$. This procedure ensures that the Hessian matrix is not excessively biased in one particular search direction and helps avoid local minima in the objective function.

For D2D-NDT, we have the additional parameter of the neighbourhood size; i.e., the number of Gaussian distributions used in the evaluation of the objective function. While our previous implementation [23] used size 0 (i.e., only the closest distribution) we currently use size 1 (i.e., the 8 neighbours in the closest layer). The other parameters (grid sizes and termination criteria) are selected in the same way as for P2D-NDT.

A similar idea, also performing registration with an objective function based on Gaussians, is used by the Generalized ICP method [21]. However, Generalized ICP assumes locally planar patches around each point, then calculates the normal direction to the local surface and uses it to bias the orientation of the covariance matrix, as opposed to P2D-NDT and D2D-NDT, which estimate the Gaussian parameters using points within a local neighborhood.

C. Plane Matching (MUMC)

The "Minimally Uncertain Maximum Consensus" (MUMC) algorithm [15] is a global alternative to the local methods like ICP and NDT. This approach consists of a pre-processing step in which plane patches are extracted from the 3D scans [25].

Especially for scenes containing man-made structures with large planar surfaces, this leads to large data-compression: the memory required for the extracted "plane-cloud" can be as small as 2.5% of the original point-cloud [16]. Each plane patch is represented by the unit normal $\hat{\mathbf{n}}$ and the distance d from the origin, along with the polygonal boundary. Using a noise model of the 3D sensor model, a 4×4 covariance matrix of the plane parameters is also computed [17] for each patch.

TABLE I: Summary of parameter selections.

	Step	Description
P2D-NDT	Data filtering of moving	grid sampling, cell size 40 cm
	Data filtering of fixed	use full point cloud
	Grid resolution	1 m, 2 m, 1 m, 0.5 m
	Termination criteria	5 iterations, $\Delta\Theta < 10^{-3}$
D2D-NDT	Data filtering (both)	use full point clouds
	Neighbor layers	1
	Grid resolution	1 m, 2 m, 1 m, 0.5 m
	Covariance scaling	$d_1 = 1, d_2 = 0.05$
	Termination criteria	5 iterations, $\Delta\Theta < 10^{-3}$
MUMC	Sensor noise model	Gaussian, $\sigma = 7$mm
	Size-similarity threshold	8
	Diversity constraint	on/off

The MUMC registration method then works directly on the two "plane clouds" corresponding to the two scans to be registered. The registration is based on finding the set of patch correspondences in the two scans which leads to the most geometrically consistent 3D transformation – as measured by the determinant of the estimated covariance matrix of the transform. This covariance is a function of the aforementioned plane-parameter covariance matrices, which in turn are a function of the sensor range noise model. Hence, a cascade of the uncertainties is maintained. The search space for correspondences can be reduced by a set of consistency tests. Some examples of these tests are: threshold for the allowable variation in the size of a given patch between scans, or patch color-histogram consistency [18], when color is available, e.g. in RGB-D scans.

MUMC also exploits the fact that for planes, the determination of rotation is decoupled from translation. Thanks to this property, combined with the vast data reduction in the number of patches compared to the number of points, and due to the pruning of the correspondence search-space by many consistency tests, MUMC can afford to do a *global, exhaustive* search for the most consistent set of patch correspondences. Hence, one of its advantages is that, unlike local methods like ICP and NDT, it does not necessarily need an initial guess for the transform. In fact, it has been shown to be able to register scans taken far away from each other and with considerable occlusion, without odometry [14].

Although the original paper [15] lists 8 parameters to be chosen, in the latest version of the algorithm only 2 parameters are selected explicitly. The others are estimated automatically based on the sensor noise-level. Since the same sensor was used for all scans in this paper, the same parameters were used for all the datasets.

- **Sensor Noise Model**: We assume Gaussian sensor noise in range measurements, with standard deviation $\sigma = 7$ mm.
- **Size-Similarity Threshold**: The determinant of the inverse of the 4×4 plane-parameter covariance matrix is proportional to N^4, where N is the number of points on the patch. The size-similarity threshold $\bar{L}_{\text{det}}$ [15] dictates the maximum allowable change in N in two potentially corresponding patches from the two scans. We set $\bar{L}_{\text{det}} = 8$, which allows the ratio of the number of points in two potentially corresponding patches to change by a factor of as much as $\exp(8/4) = 7.4$. This is a very permissive value.

In addition to the above numerical parameters, MUMC can be run in two modes, as explained below.

The Plane Diversity Constraint (DC): For MUMC to compute translation reliably, it needs to find plane correspondences in all directions. When only two or less translation components can be found reliably (e.g., the corridors in the ETH dataset desribed

below) the uncertainty is automatically detected by MUMC because a certain matrix is effectively numerically rank-deficient [15, Eq. (25)].

In this case, there are two options for MUMC:

- **DC-OFF**: This option signals that we want to keep the rotation estimate and the reliably found translation components. For the translation component in the unreliable direction, we could either set it to zero or, if available, we could use the odometry component in that direction. In both cases, the error in this direction will be large and this will adversely affect the translation accuracy statistics of the algorithm.
- **DC-ON**: In this case, MUMC automatically declares the registration as having failed rather than venturing to fill-in unavailable translation components with heuristics or odometry. This result will then not be considered for computing the accuracy statistics.

D. ICP

The iterative closest point (ICP) algorithm was first introduced in 1991 [5] and is still widely used for registration of 3D point clouds. The two seminal papers on ICP were written by Besl and McKay [1] and Chen and Medioni [5]. To summarize the algorithm concisely: ICP iteratively refines the relative pose of two overlapping scans by minimizing the sum of squared distances between corresponding points in the two scans. Corresponding point pairs are identified either by Euclidean point-to-point distance [1] or by a point-to-plane metric [5], which measures the distance from a point in one scan and the closest tangent plane in the other. Since its conception, a large number of variants have been developed, differing in, e.g., how points are selected and how to select point-to-point correspondences. However, the main structure of the algorithm remains. The point-to-plane variant has been shown to be more accurate in many cases, and Pomerleau et al. [20] show that it also performs better for the benchmark used here. As specified in the experimental protocol, we compare our algorithms to the baseline implementation of the well-established point-to-plane ICP variant.

The parameter selection for ICP is the same as in [20].

IV. Data and protocol

We have used the same six environments from the "Challenging Laser Registration" data sets [19] as in Pomerleau et al. [20]. One of the main advantages of these data sets is that the ground-truth poses of all point clouds have been tracked with millimeter precision using a total station. These six data sets cover both indoor and outdoor environments, cluttered and open, some with large planes and some with more variable surfaces.

Apartment: An apartment with five rooms. This data set has denser scans than the others: 365 k points per scan, compared to 100 k–200 k for the others. (See Fig. 1a–1b.)

Stairs: A staircase transitioning from indoor to outdoor.

ETH: Large hallway with pillars and arches. These scans have little constraints along the direction of the hallway, and also features repetitive structures in the form of the pillars.

Gazebo (winter): A public park with a gazebo.

Wood (summer): Dense vegetation around a small path.

Plain: Open field atop a mountain in the Alps. Includes very little geometric structure. (See Fig. 1c–1d.)

The data sets come with sets of initial pose offsets, to be used for assessing the algorithms' robustness to poor initial pose estimates. These pose offsets are indeed quite challenging, and a large part of them are much worse than what can be expected to be encountered by a mobile robot. The offsets categorized as "easy", "medium", and "hard", and are generated from zero-mean normal distributions, where the standard deviation is larger for the more difficult categories. The "easy" poses have a standard deviation of 0.1 m and 10°, while the "hard" poses have a standard deviation of 1.0 m and 45°. Although the translation offsets are not so severe, the rotation offsets are very large. Some of the "hard" poses have an initial rotation offset of more than 90°. This is very challenging for any local registration algorithm, which may more likely converge to a solution that is rotated 180° than the correct orientation. Even some of the "easy" poses are offset more than 30°, which is not particularly easy – especially not for scan pairs with little overlap from unstructured environments. Conversely, some of the "hard" poses may be quite close to ground truth.

A. Suggested amendments to the protocol

For future work, we suggest the following amendments to the protocol [20].

1) Fixed-magnitude pose offsets: The pose offsets should have fixed magnitudes (as in Magnusson et al. [11]) rather than being sampled from normal distributions with increasing variance. Given the scale of the scans, reasonable magnitudes might be 0.5 m and 10° for "easy" poses, 2.5 m and 20° for "medium" poses, and 5 m and 45° for "hard" poses.

2) More unique scan pairs: The large number of initial pose estimates are relevant only to the local methods. For global methods which do not necessarily need initial guesses, it is more important to have more unique pairs and their ground-truth transforms.

V. Results

The results of our evaluations are summarised in Figs. 2 and 3. The rotation and translation errors are plotted separately, but precise registrations should have small errors both in translation and rotation. Due to space constraints, we were not able to include plots about all pertinent aspects of the benchmark. The complete outcome[2] for the NDT-based methods, as well as additional tables and plots of the results[3] are available online.

For the local registration methods (ICP and the NDT-based methods), we provide separate plots for the scan pairs with "easy" pose perturbations only (Fig. 3c) and the large overlaps only (Fig. 3b), in addition to plots for the complete data sets (Fig. 3a).

Because MUMC does not make use of an initial estimate, the only relevant sub-category is the amount of overlap. Another consequence is that the statistics are computed only from the 35 unique scan pairs from each data set, as opposed to 6720 combinations of scan pairs and pose offsets for the local registration methods. In addition to the magnitude of the final pose error, the entries for MUMC also specifies the percentage of scans that were used to compute the errors. The remaining percentage of scans could not be registered, but were also successfully declared as having failed.

A. Accuracy

The accuracy of the final solution (after registration) is measured as described in Pomerleau et al. [20, Eqs. 1–3]. The translation error is the Euclidean norm of the difference between the ground-truth and the output translation vectors. The rotation error is defined as the geodesic distance from the rotation matrix that brings the moving point cloud from the output orientation to that of the ground-truth pose. Error statistics are discussed in terms of quantiles where Q50 is the median and Q95 is the 95th percentile.

[2] http://projects.asl.ethz.ch/datasets/doku.php?id=laserregistration:evaluations:home

[3] http://aass.oru.se/Agora/Benchmarks/

The unstructured data sets, Wood and Plain, are quite difficult for all of the algorithms. Because they do not contain enough geometric structure, they are challenging for MUMC in particular. Looking at the percentages of matches estimated by MUMC to be successful, we can see that it detects that it is not able to perform matching in most cases. For Wood, MUMC detects a lack of features in 86% of the 35 scan pairs with DC-ON (63% with DC-OFF), and only tries to match the remaining 5 pairs, which means 14% of the pairs from this dataset. Because of the lack of structure, the translation error is above 50 cm also for the remaining pairs.

For Wood scans with large overlap (over 75%) ICP is accurate (less than 10 cm error) up to Q50, while P2D-NDT is equally accurate up to Q75. P2D-NDT is the only algorithm that is able to register any outdoor scans with small overlap (30%–50%), and is significantly better than the others for the Plain dataset (accurate to Q50 for "easy" poses). D2D-NDT performs similarly to ICP for the unstructured data sets.

Gazebo is an outdoor data set, but it also contains a prominent built structure. In fact, this data set proved slightly easier than the indoor data sets for the NDT methods, judging by Fig. 3a. We believe that the reason for this is in the combination of large surfaces that the moving scans can "slide on" and good constraints from the gazebo itself, which are not planar enough to be useful for MUMC.

For the structured data sets (including Gazebo), P2D-NDT finds accurate solutions up to at least Q75 as long as the pose offset is "easy", and about Q45–Q55 for all poses. This is in contrast to ICP, which finds accurate solutions up to Q50 for the "easy" poses, and Q30–Q40 for the all poses. Another finding is that D2D-NDT has better overall accuracy for the complete datasets, but when looking at the "easy" poses only, P2D-NDT is better. In other words, D2D-NDT is less sensitive to poor initial pose estimates but sometimes less precise when a good pose estimate is available.

MUMC performs much better for Apartment and Stairs than the other datasets, because it can exploit the structure. Stairs in particular works well. Counting the pairs that the algorithm flags as successfully matched, MUMC DC-ON correctly registers 100% of the pairs with large overlap from that dataset, and 95% of all pairs. ETH, on the other hand, is difficult because it only has a strong planar component along one direction. MUMC finds the correct *orientation* in most cases, or detects that it cannot provide a certain result (see Fig. 2b).

Some of the "easy" poses are also quite difficult for the local methods. Practically no registrations converge to an acceptable solution for all these cases. The exception is P2D-NDT on the Gazebo dataset, with accurate solutions (within 5 cm and 2° from ground truth) even at the 95th percentile for the "easy" poses.

Comparing Figs. 3a and 3b, it can be seen that ICP is more sensitive to small overlaps than the NDT-based methods. Considering only scan pairs with large overlap, ICP's results are more similar to NDT's than when considering the "easy" poses only. NDT often succeeds up to at least Q25 also small overlaps (30%–50%), although scan pairs with small overlap from the unstructured datasets are very challenging, especially for D2D-NDT. As long as there is diverse enough planar structure in the environment, which is the case in Apartment and Stairs, MUMC is quite robust to small overlap ratios, which can be seen by the fact that the corresponding curves in Figs. 3d and 3e are similar.

B. Further discussion of MUMC results

The most important aspect of the MUMC results is that since MUMC is a global method, *no initial guess* was provided to it. The only categorisation pertinent to MUMC is the overlap level: large (easy to register), medium, and small (difficult to register). As noted above, the local algorithms (NDT and ICP) do require an initial guess that is close enough to the true solution.

In addition to the converged 3D transform, MUMC also returns a flag for whether the result can be considered successful (based on the number of correspondences found) and a covariance matrix of the transform.

The percentage of matches labelled by MUMC as successful is noted for each dataset in the plots. The stricter MUMC DC-ON will also consider a registration unsuccessful if certain components of translation cannot be found, as explained in Sec. III-C. Therefore, the success percentage of MUMC DC-ON for each dataset is less or equal to that of MUMC DC-OFF.

The covariance matrix of the transform clearly shows the dominant uncertain directions (the eigenvectors corresponding to high eigenvalues). It is clear from Fig. 2b that the rotation determination of both MUMC DC-ON and DC-OFF is very accurate for the cases that are flagged as successful – in particular for the ETH dataset.

At this point it should be noted that the Hessian of the NDT score function (2), (3) can also be used to construct a covariance estimate of the pose after registration, in order to flag unsuccessful matches [8, 22]. A detailed analysis of that is not within the scope of the present paper, but is a topic of ongoing work.

C. Timing

The execution times when running the benchmark are summarized in Figure 3. The reported times include all pre-processing (extracting plane patches for MUMC, building NDT representations, constructing kd-trees for ICP, etc.) but exclude the time required for loading the scan files from disk.

As aptly noted by Pomerleau et al. [20], it is difficult to make precise comparisons of execution times. Many uncertainties affect execution time: not only the hardware used, but also the compiler, the skill of the programmers, etc. The execution times provided here can only give a coarse estimate of the speed.

The execution times were measured on different computers. NDT was running on a quad-core 3.50 GHz Intel Core i7 CPU. MUMC was running on an 3.40 GHz Intel Core i7. Please note that these are slightly faster computers than the 2.2 GHz Core i7 used for ICP [20].

Although the implementations can make use of multiple cores, for these tests they were all running in a single thread. Typically four batches were being run in parallel (each on a separate CPU core) to reduce the overall processing time.

Implementation details: The difference between the execution speed of ICP and P2D-NDT is smaller than what has been reported in our earlier publications. One of the reasons is that the ICP implementation used here (libpointmatcher[4]) uses more efficient components (e.g., the kd-tree implementation, where most of the execution time for ICP is spent, uses libnabo instead of libann).Another reason is that the old P2D-NDT implementation[5] runs significantly faster than this version, from `perception_oru`. Most likely, this is because the old implementation uses the OPT++ library for the central optimization loop, while `perception_oru` uses its own optimization implementation. However, our tests with the old implementation has shown that it often is trapped in local minima when used in this benchmark, which results in poorer accuracy.

[4]https://github.com/ethz-asl/libpointmatcher

[5]http://aass.oru.se/~mmn/software/ndt_test_suite_v0.1.zip

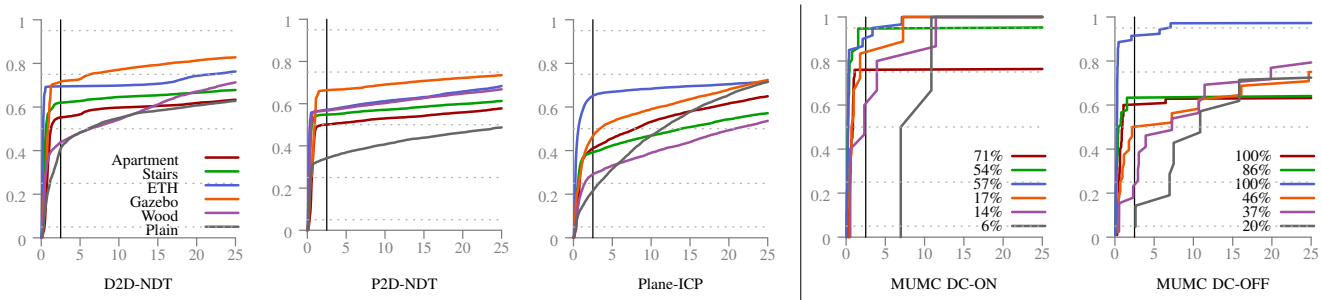

(a) Cumulative probabilities of rotation errors for NDT and ICP, for all types of poses and overlaps.

(b) Cumulative probabilities of rotation errors for MUMC. No initial pose was given.

Fig. 2: Cumulative probability plots of rotation errors after registration. Rotation error (in degrees) is on the horizontal axis. The MUMC plots also include the percentage of scan pairs from which the plots are generated. A suggested threshold for successful matches (2.5°) is marked with a vertical bar.

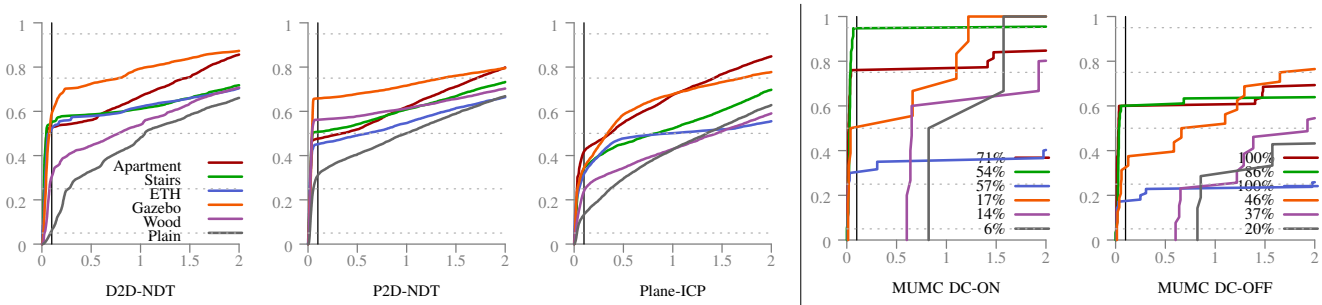

(a) Cumulative probabilities of translation errors for NDT and ICP, for *all types of poses and overlaps*.

(d) Cumulative probabilities of translation errors for MUMC, for *all scan pairs*. No initial pose was given.

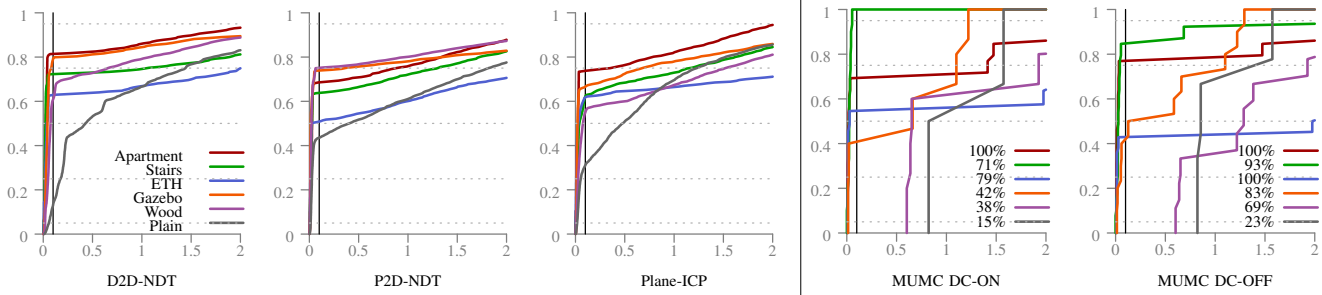

(b) Cumulative probabilities of translation errors for NDT and ICP, *for large overlaps* (over 75%) but all poses.

(e) Cumulative probabilities of translation errors for MUMC, for *large overlaps*. No initial pose was given.

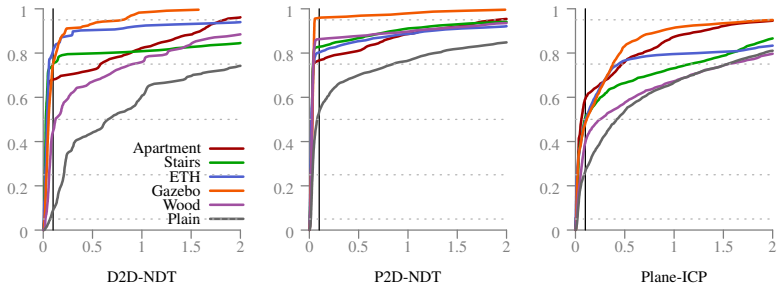

(c) Cumulative probabilities of translation errors for NDT and ICP, *for "easy" poses*, but all levels of overlaps.

Statistics of execution times, for all data sets.

Algorithm	CPU	Q50	Q95
Plane ICP	i7 2.2 GHz	2.58 s	8.43 s
P2D-NDT	i7 3.5 GHz	1.48 s	8.75 s
D2D-NDT	i7 3.5 GHz	0.37 s	0.82 s
MUMC DC-OFF	i7 3.4 GHz	2.95 s	18.01 s
MUMC DC-ON	i7 3.4 GHz	2.41 s	12.95 s

Fig. 3: Cumulative probability plots of translation error after registration. Cumulative probabilities are on the vertical axes. Translation error (m) is on the horizontal axis, On the left are plots for the local methods (NDT and ICP), and on the right are plots for the global methods. The MUMC plots also include the percentage of scan pairs from which the plots are generated. A suggested threshold for successful matches (10 cm error) is marked with a vertical bar.

VI. Conclusions and future work

Judging by the results summarized in Figs. 2–3, which is the result of over 120 000 scan matches, we conclude that MUMC and NDT generally provides more robust registration than point-to-point or point-to-plane ICP when faced with scan pairs that have either small overlap or a poor initial alignment. Plots for point-to-point ICP have been omitted due to space constraints. The main advantage of MUMC is that it performs well even when no initial pose estimate (from odometry) is available, as long as there is sufficient structure in the environment. The two NDT-based methods (P2D-NDT and D2D-NDT) do require initial estimates, but are much less sensitive to errors in this estimate than ICP. D2D-NDT and, in particular, P2D-NDT work better than MUMC outdoors, because they have less strict assumptions on planarity. D2D-NDT is the fastest of the evaluated methods, with a median execution time that is about 7 times shorter than non-NDT methods.

For situations where no initial pose estimate is available, MUMC provides a good solution in common indoor environments, and can also provide information about whether it has successfully matched two 3D scans or not. For real-time use on a robot, D2D-NDT is preferable because of its faster execution speed. For challenging data sets with little structure or little overlap, P2D-NDT provides the best accuracy.

The benchmark protocol used here was designed for local registration methods. In future work, we will adapt the benchmark to more fairly assess the performance also of global methods, by including more unique pairs of scans from the given datasets.

Generating datasets of similar quality (with precise 6-DOF ground truth poses) for other sensors types (e.g. Velodyne scanners or RGB-D cameras) and environments would also be very useful.

More sophisticated algorithms also return the covariance of the registration transform in addition to the transform itself. Some way to automatically assess the accuracy of this estimation, at least in terms of the primary uncertainty directions would be useful.

References

[1] Paul J. Besl and Neil D. McKay. "A Method for Registration of 3-D Shapes". In: *IEEE Trans. Pat. Analysis and Mach. Intelligence* 14.2 (Feb. 1992), pp. 239 –256.

[2] Peter Biber and Wolfgang Straßer. "The Normal Distributions Transform: A New Approach to Laser Scan Matching". In: *IROS*. Las Vegas, USA, Oct. 2003, pp. 2743–2748.

[3] Peter Biber, Sven Fleck, and Wolfgang Straßer. "A Probabilistic Framework for Robust and Accurate Matching of Point Clouds". In: *26th Pattern Recognition Symposium (DAGM 04)*. 2004.

[4] Simone Ceriani, Giulio Fontana, Alessandro Giusti, Daniele Marzorati, Matteo Matteucci, Davide Migliore, Davide Rizzi, Domenico G. Sorrenti, and Pierluigi Taddei. "RAWSEEDS ground truth collection systems for indoor self-localization and mapping". In: *Autonomous Robots* 27 (2009), pp. 353–371.

[5] Yang Chen and Gérard Medioni. "Object modeling by registration of multiple range images". In: *ICRA*. 1991, pp. 2724–2729.

[6] A Das and S.L. Waslander. "Scan registration with multi-scale k-means normal distributions transform". In: *IROS*. 2012, pp. 2705–2710.

[7] Andrew Howard and Nicholas Roy. *The Robotics Data Set Repository (Radish)*. 2003. URL: http://radish.sourceforge.net/.

[8] Martin Magnusson. "The Three-Dimensional Normal-Distributions Transform — an Efficient Representation for Registration, Surface Analysis, and Loop Detection". Örebro Studies in Technology 36. PhD thesis. Örebro University, Dec. 2009.

[9] Martin Magnusson and Tom Duckett. "A Comparison of 3D Registration Algorithms for Autonomous Underground Mining Vehicles". In: *ECMR*. Ancona, Italy, Sept. 2005, pp. 86–91.

[10] Martin Magnusson, Andreas Nüchter, Christopher Lörken, Achim J. Lilienthal, and Joachim Hertzberg. "Evaluation of 3D Registration Reliability and Speed — A Comparison of ICP and NDT". In: *ICRA*. Kobe, Japan, May 2009, pp. 3907–3912.

[11] Martin Magnusson, Achim J. Lilienthal, and Tom Duckett. "Scan Registration for Autonomous Mining Vehicles Using 3D-NDT". In: *J. Field Robotics* 24.10 (Oct. 2007), pp. 803–827.

[12] Niloy J. Mitra, Natasha Gelfand, Helmut Pottmann, and Leonidas Guibas. "Registration of Point Cloud Data from a Geometric Optimization Perspective". In: *Proceedings of the Symposium on Geometry Processing*. 2004, pp. 22–31.

[13] Andreas Nüchter and Kai Lingemann. *Robotics 3D Scan Repository*. 2011. URL: http://kos.informatik.uni-osnabrueck.de/3Dscans/.

[14] Kaustubh Pathak, Dorit Borrmann, Jan Elseberg, Narunas Vaskevicius, Andreas Birk, and Andreas Nüchter. "Evaluation of the Robustness of Planar-Patches based 3D-Registration using Marker-based Ground-Truth in an Outdoor Urban Scenario". In: *IROS*. Taipei, Taiwan, 2010, pp. 5725–5730.

[15] Kaustubh Pathak, Andreas Birk, Narunas Vaskevicius, and Jann Poppinga. "Fast Registration Based on Noisy Planes With Unknown Correspondences for 3-D Mapping". In: *Robotics, IEEE Transactions on* 26.3 (2010), pp. 424–441. ISSN: 1552-3098.

[16] Kaustubh Pathak, Andreas Birk, Narunas Vaskevicius, Max Pfingsthorn, Sören Schwertfeger, and Jann Poppinga. "Online Three-Dimensional SLAM by Registration of Large Planar Surface Segments and Closed-Form Pose-Graph Relaxation". In: *Journal of Field Robotics* 27.1 (2010), pp. 52–84.

[17] Kaustubh Pathak, Narunas Vaskevicius, and Andreas Birk. "Uncertainty analysis for optimum plane extraction from noisy 3D range-sensor point-clouds". English. In: *Intelligent Service Robotics* 3.1 (2010), pp. 37–48. ISSN: 1861-2776.

[18] Kaustubh Pathak, Narunas Vaskevicius, Francisc Bungiu, and Andreas Birk. "Utilizing Color Information in 3D Scan-Registration Using Planar-Patches Matching". In: *IEEE Int. Conf. on Multisensor Fusion and Information Integration*. Hamburg, 2012.

[19] François Pomerleau, M. Liu, Francis Colas, and Roland Siegwart. "Challenging data sets for point cloud registration algorithms". In: *IJRR* 31.14 (Dec. 2012), pp. 1705–1711.

[20] François Pomerleau, Francis Colas, Roland Siegwart, and Stéphane Magnenat. "Comparing ICP Variants on Real-World Data Sets". In: *Autonomous Robots* 34.3 (Apr. 2013), pp. 133–148.

[21] A. Segal, D. Haehnel, and S. Thrun. "Generalized-ICP". In: *Proceedings of Robotics: Science and Systems*. Seattle, USA, 2009.

[22] Todor Stoyanov. "Reliable Autonomous Navigation in Semi-Structured Environments using the Three-Dimensional Normal Distributions Transform (3D-NDT)". PhD thesis. Örebro university, 2012.

[23] Todor Stoyanov, Martin Magnusson, and Achim J. Lilienthal. "Fast and Accurate Scan Registration through Minimization of the Distance between Compact 3D NDT Representations". In: *IJRR* 31.12 (12 2012), pp. 1377–1393.

[24] Todor Stoyanov, Martin Magnusson, and Achim J. Lilienthal. "Point Set Registration through Minimization of the L2 Distance between 3D-NDT Models". In: *ICRA*. 2012.

[25] Narunas Vaskevicius, Andreas Birk, Kaustubh Pathak, and Soren Schwertfeger. "Efficient Representation in 3D Environment Modeling for Planetary Robotic Exploration". In: *Advanced Robotics* 24.8-9 (2010), 1169—1197.

[26] O. Wulf, A. Nüchter, J. Hertzberg, and B. Wagner. "Benchmarking urban six-degree-of-freedom simultaneous localization and mapping". In: *J. Field Robotics* 25 (2008), pp. 148–163.